A random walk description of the heterogeneous glassy dynamics of attracting colloids

Pinaki Chaudhuri[1], Yongxiang Gao[2], Ludovic Berthier[1], Maria Kilfoil[2], and Walter Kob[1]

[1] Laboratoire des Colloïdes, Verres et Nanomatériaux, UMR 5587, Université Montpellier II and CNRS, 34095 Montpellier, France
[2] Department of Physics, McGill University, Montréal, Canada H3A 2T8

E-mail: berthier@lcvn.univ-montp2.fr

Abstract. We study the heterogeneous dynamics of attractive colloidal particles close to the gel transition using confocal microscopy experiments combined with a theoretical statistical analysis. We focus on single particle dynamics and show that the self part of the van Hove distribution function is not the Gaussian expected for a Fickian process, but that it reflects instead the existence, at any given time, of colloids with widely different mobilities. Our confocal microscopy measurements can be described well by a simple analytical model based on a conventional continuous time random walk picture, as already found in several other glassy materials. In particular, the theory successfully accounts for the presence of broad tails in the van Hove distributions that exhibit exponential, rather than Gaussian, decay at large distance.

PACS numbers: 64.70.Pf, 05.20.Jj

1. Dynamic heterogeneity in colloidal gels

There are many systems in nature whose dynamics become slow in some part of their phase diagram, because they undergo a transition from a fluid to a disordered solid phase — like in a sol-gel transition, a glass transition, or a jamming transition. These systems are generically called "glassy materials", examples of which are simple or polymeric liquids, colloidal particles with soft-core or hard-core interactions, grains, etc. As physicists, we would like to have a microscopic understanding of the slow dynamics of these materials and would like to answer, in particular, an apparently very simple question: How do particles move in a glassy material close to the fluid-solid transition? To answer this question directly, one needs to resolve the dynamics of individual particles. In experiments, this is a particularly hard task for molecular liquids, although some techniques are now available [1, 2] but becomes much easier in the colloidal and granular worlds, where direct visualization is possible [3, 4, 5, 6, 7, 8, 9, 10]. Of course, resolving single particle dynamics is trivial in computer simulations where, for each particle in the system, the equations of motion are directly integrated.

Hence, single particle dynamics have now been well documented, both numerically and experimentally, in a wide variety of materials. A most striking feature emerging from these studies is the existence of dynamic heterogeneity [11]. In terms of single

particle trajectories, dynamic heterogeneity implies the existence of relatively broad distributions of mobilities inside the system. It is therefore an important task to suggest a framework to describe and interpret those data, and hopefully understand the physical content carried by single particle displacements.

In this work, we study an assembly of moderately attractive colloidal particles (attraction depth $U \approx 3k_BT$, where k_BT is the thermal energy) that undergo dynamic arrest at an "intermediate" volume fraction, $\phi_c \sim 0.44$ [9]. The system is in fact intermediate between fractal gels made of very strongly attractive particles ($U \gg k_BT$) at very low volume fraction, and hard sphere glasses obtained with no attraction ($U \approx 0$) at a much higher volume fraction, $\phi \approx 0.6$. Although experiments clearly detect the presence of an amorphous phase with arrested dynamics, the nature of the transition towards this "dense gel" (or low density glass!) remains unclear [12]. The transition seems too far from the so-called "attractive glass" obtained at higher volume fraction in colloids with very short-range attraction (sticky particles), so that other phenomena are usually invoked. A popular hypothesis is that gelation is in fact a non-equilibrium phenomenon due to a kinetically arrested phase separation [12, 13]. Dynamic heterogeneity in such systems has been analyzed before in just a few systems, both experimentally [9, 10] and numerically [14, 15].

In this paper, we analyze single particle dynamics on the approach to the glassy phase and show that the self-part of the van Hove distribution function is not the Gaussian expected for a Fickian process, but that it reflects instead the existence, at any given time, of colloids with widely different mobilities: Our system is dynamically heterogeneous. We then show that the simple analytical model proposed in Ref. [16] to describe data in a variety of systems close to glass and jamming transitions also describes our experimental data in a satisfactory manner.

This paper is organized as follows. In Sec. 2 we describe the system, experimental techniques, and the results obtained for the van Hove function. In Sec. 3 we describe the model used to fit the experimental data and discuss the results. We conclude the paper in Sec. 4.

2. Measuring single particle dynamics using confocal microscopy

2.1. Experimental system and techniques

The experimental system under study is a suspension of colloidal particles interacting through a hard-core repulsion and a softer attractive interaction, induced by depletion by adding polymers. Details of the system have been presented in Ref. [9]. The dynamics of this system is observed using confocal fluorescence microscopy. The strength of the inter-particle attractive interaction, U, is determined by the concentration of polymers in the suspension. We present data for a sample at a moderate interaction strength of $U \approx 2.86k_BT$. We work at constant temperature T, so that our control parameter is the volume fraction of the particles, ϕ. We find that the system becomes a gel when ϕ is increased, with a transition close to $\phi_c \approx 0.442$ [9]. Measurement of different relevant statistical quantities are carried out at different $\phi < \phi_c$.

Our procedure to vary slowly the volume fraction uses particle sedimentation. The relative buoyancy of the colloids is $\Delta\rho = 0.011$ g/cm^3, corresponding to a gravitational height of $h = k_BT/(\frac{4}{3}\pi a^3 \Delta\rho g) \approx 40$ particle radii a, where g is the acceleration due to gravity. Therefore, the gravitational field is small enough that it induces a very

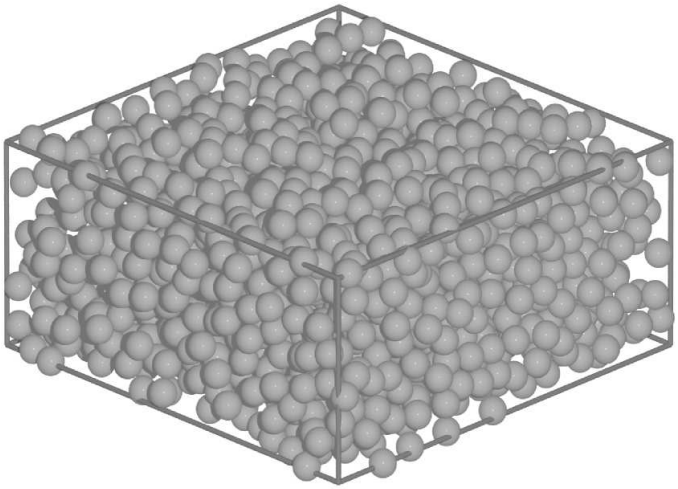

Figure 1. Three-dimensional confocal microscopy rendered image of a typical particle configuration at volume fraction $\phi = 0.429$.

slow densification of the system. The densification is slow enough that microscopic dynamics of the colloids remains controlled by the interplay between attraction and steric hindrance, rather than by sedimentation itself. Moreover, the large asymmetry between polymer coil diffusion time, ≈ 0.3 s, and particle sedimentation time over one particle, ≈ 260 s, ensures that polymers are uniformly distributed, maintaining the interaction strength U constant in the course of the experiment.

The colloidal particles are polymethyl-methacrylate (PMMA) spheres of diameter 1.33 μm, sterically stabilized by chemically grafted poly-12-hydroxystearic acid, dyed with the electrically neutral fluorophore 4-chloro-7-nitrobenzo-2 oxa-1,3-diazole (NBD), and suspended in a solvent mixture of decahydronaphthalene (decalin), tetrahydronaphthalene (tetralin), and cyclohexyl bromide (CXB) that allows for independent control of the refractive index and buoyancy matching with the particles. Polystyrene polymers (molecular weight 11.4×10^6 g/mol) are added at 1.177 mg/ml to induce a depletion attraction at a range estimated by $\Delta = 2R_g = 0.28a$, where R_g is the polymer radius of gyration.

Using confocal microscopy, we collect stacks of images at fixed time intervals ranging from 12 to 1500 s at different ϕ to access short and long time dynamics during the approach to gelation. From the stacks of images we extract the particle positions of 10^3 particles in three dimensions and track their positions at better than 10 nm resolution over time. A three-dimensional rendering of a typical particle configuration from a stack of images at $\phi = 0.429$ is illustrated in Fig. 1.

2.2. Non-Gaussian distributions of single particle displacements

In an earlier work [9], we analyzed some structural and dynamical properties of the system for different volume fractions. In particular, we analyzed in some detail the distinct part of the van Hove function, finding dynamic signatures typical of gel systems. We only presented briefly some preliminary results concerning the self-part

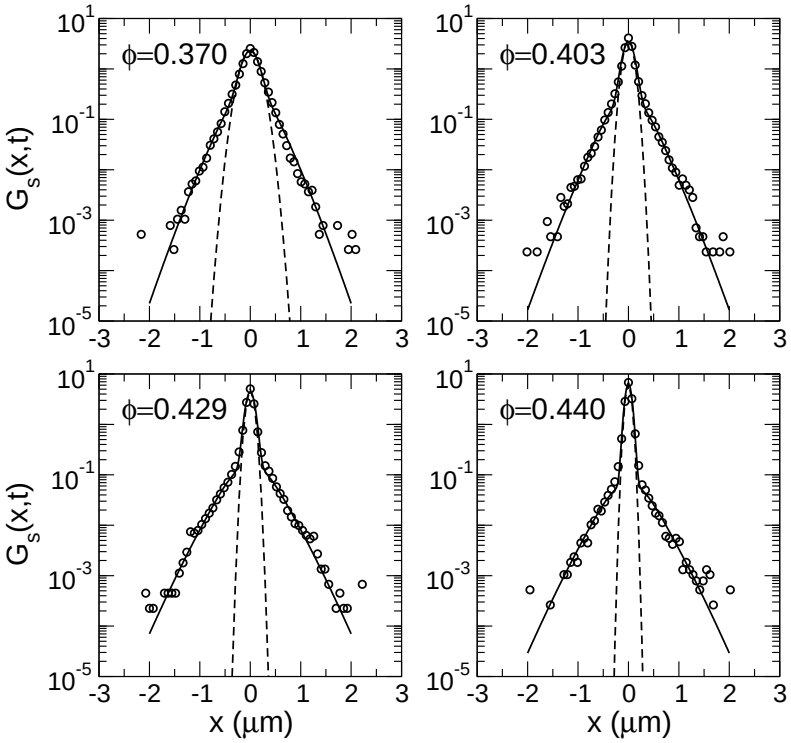

Figure 2. The self-part of the van Hove function, Eq. (1), measured using confocal microscopy upon approaching the colloidal gel transition by increasing the volume fraction ϕ. For each ϕ we show the distribution for a time corresponding to average particle displacements being close to the particle radius. Dashed lines represent Gaussian fits to the center of the distribution. The full lines through the data are fits obtained from the model and parameters described in Sec. 3, showing very good agreement with the data.

of the van Hove function. It is the latter that we investigate in more detail here. It is defined by

$$G_s(x,t) = \frac{1}{N}\sum_{i=1}^{N} \delta(x - [x_i(t) - x_i(0)]), \tag{1}$$

where $x_i(t)$ denotes the position of particle i at time t along one of the horizontal directions. The function $G_s(x,t)$ measures the probability that a given particle has undergone a displacement x in a time interval of duration t.

Once the distribution (1) is known, several quantities can be determined. Perhaps the simplest one is the mean squared displacement, $\langle x^2 \rangle$, where the average is taken over the distribution $G_s(x,t)$, which contains quantitative information about the average mobility of the colloidal particles. In particular, its long-time limit yields values for the self-diffusion constant D_s of the particles through $\langle x^2 \rangle \sim 2D_s t$ for large t. Such a measurement, however, tells nothing about the possible presence of dynamic heterogeneity in the system.

In our earlier study [9], we had measured $\langle x^2 \rangle$; although we observed a slowing down of the dynamics, the heterogeneous nature remains hidden and could only

be seen by measuring $G_s(x,t)$. In Fig. 2, we have plotted $G_s(x, t \sim t^\star)$ for four different volume fractions ranging from 0.37 to 0.44, where $t^\star$ corresponds to the time when $\sqrt{\langle x^2 \rangle} \approx 0.2a$ (a being the particle radius) - which is a meaningful measure of the timescale for structural relaxation [9]. We can clearly see that $G_s(x,t)$, at this timescale, is very non-Gaussian and therefore, the particle trajectories do not correspond to Fickian dynamics.

It can be easily seen that although, in all four cases, most of the statistical weight of the functions is carried by particles which have barely moved, $x < 0.5\mu$m, there is a pronounced tail extending to distances that are much larger than what is expected for the Gaussian prediction shown as dashed lines [9]. The small x behavior, however, is not far from a Gaussian distribution, corresponding to quasi-harmonic vibrations in the cage formed by neighbouring particles, but at large distances the decay is well described by an exponential, rather than a Gaussian, decay. Thus, the single particle motion for our experimental system at timescales corresponding to $t^\star$ is strongly non-diffusive. Such a non-Gaussian behaviour has been observed in other glass-forming systems, both in simulations [17, 18, 19] and experiments [3, 4, 5, 6, 7].

Such non-Gaussianity is related to the presence of heterogeneity in the dynamics of the particles in the system. Most of the particles simply undergo vibrational motion around their initial position — this corresponds to the central Gaussian part in $G_s(x,t)$. Additionally, a small fraction of the particles gets the opportunity to explore larger distances during the observational time and contributing to the non-trivial tail of $G_s(x,t)$ [17]. Moreover, Fig. 2 shows that, with increasing volume fraction, the width of the central Gaussian of $G_s(x,t)$ at time $t^\star$ decreases while the tail gets more pronounced. This implies that even though the volume available for the quasi-harmonic vibrations decreases with ϕ, some particles still find pathways to travel large distances and allow the structural relaxation of the system.

Several attempts have been previously made to empirically fit the non-Gaussian shape of $G_s(x,t)$ with known functional forms. Weeks *et al.* [4] have tried to fit their experimentally measured $G_s(x,t)$ with a stretched exponential function, in order to fit both the broad tails and the narrow center. Attempts have also been made to fit both components of the van Hove function as the sum of two different Gaussian functions [3, 9]. However, neither attempts seem to give satisfactory results since the shape of the distribution changes with time. Basing their analysis on numerical simulations of a Lennard-Jones system, Stariolo and Fabricius [18] recognized that the tails are probably better fitted with an exponential function in some time window. Using extensive data, it has recently been shown [16] that the $G_s(x,t)$, for different glass-formers, colloidal hard spheres and granular materials close to jamming are better represented by a superposition of a central Gaussian along with an exponential tail for the large distances, which crosses over, at large times, to a Gaussian form. The model therefore allows one to describe the data at different times without changing the fitting formula in the middle of the game. As we show below, the exponential tail is interpreted as the direct consequence of the occurrence of rare events of particles undergoing large displacements that are statistically distributed.

3. Random walk analysis

3.1. Modeling single particle dynamics

There have been several attempts to map the heterogeneous single particle dynamics of gels and glass-formers to some stochastic process. Closely related to our approach are the ones of Refs. [19, 20, 21]. Odagaki and Hiwatari [19] have studied the dynamics of atoms near the glass transition of simple classical liquids, on the basis of a mesoscopic stochastic-trapping diffusion model, and calculated various dynamical quantities such as the mean squared displacement, non-Gaussian parameter and intermediate scattering functions. Monthus and Bouchaud [20] have looked at various models of independent particles hopping between energy traps which have relaxation functions similar to glass-formers. They also show that diffusion in trap models can be described using the formalism of the continuous time random walk (CTRW) [22], widely used in many different areas of physics. Finally, Berthier *et al.* [21] also proposed to describe the process of self-diffusion in glass-forming materials in terms of a CTRW picture, and they base their analysis on the study of spin facilitated models. In this context, the CTRW picture directly follows quite generically from the spatially heterogeneous nature of the dynamics [23] .

In fact, a convincing empirical rationale for this type of approaches stems from a visual inspection of particle trajectories in materials with slow dynamics, such as the ones shown in both panels of Fig. 3, which represent examples of particle displacements for a Lennard-Jones supercooled liquid [24] and for the present colloidal system. Direct visualization reveals that, when observed on a timescale comparable to $t^\star$, most of the particles simply perform a large number of localized vibrations around their initial position, just as in a disordered solid. However, the particles that contribute to the tail of the van Hove function undergo one or several quasi-instantaneous jumps separating long periods of localized vibrations, as can be seen in Fig. 3. For both systems, we observe that these jumps occur randomly in time and also have distributed amplitudes. Therefore, a continuous time random walk [22] should be a good coarse-grained stochastic model for single particle trajectories of these systems as suggested before [19, 20, 21, 23].

The case of very low density gels is peculiar, since in these systems there is a well-defined network of quasi-immobile particles existing along with the free particles. Therefore, the system can truly be decomposed into two dynamically distinct families, whose properties directly follow from the heterogeneous nature of the stucture of these gels. Indeed, a two-family dynamical model has been shown to fit the van Hove distribution functions obtained in computer simulations of gel systems for a wide window of parameters [15]. However, for denser systems, we have no structural basis to assume that such a distinction can be made, although this has been done in other studies [25]. For supercooled liquids, it can even be quantitatively established by simulations [26] that dynamic heterogeneity at the particle scale has no such structural origin. Since the present system lies somewhat in between low density gels and dense glasses, it is not obvious *a priori* whether we should adopt a glass (one family) or a gel (two families) description. In fact, we will show that the strong hypothesis of a two-family model is not necessary to account for our measurements. Therefore we will model the system as a collection of indistinguishable particles undergoing continuous time random walks and we prove below that such a modeling accounts well for the data presented in Fig. 2. Obviously, a two-family model would also fit our data very

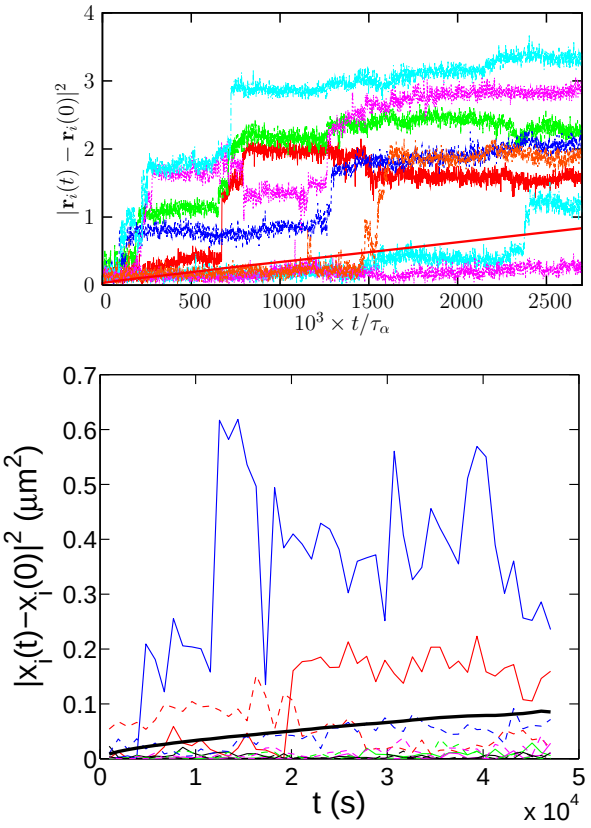

Figure 3. Temporal evolution of squared displacement from an initial position for (top) particles in a binary Lennard Jones liquid at low temperature, $T = 0.435$ (top), and (bottom) for the attractive colloidal particles at $\phi = 0.429$. While some particles rattle around their mean position, others perform one or several quasi-instantaneous jumps. Occurrence of jumps occur randomly in time and are random in size. The straight line in the plots corresponds to the mean-squared displacement.

well since one can always artificially separate one group of particles into two distinct subgroups, (the reverse is not necessarily true).

3.2. A simplified CTRW model

We now describe the CTRW model, introduced in Ref. [16], which will be used to fit the experimental data. We consider particles undergoing a stationary, three-dimensional, isotropic random walk process, as in the original Montroll-Weiss CTRW model [22], and add to the process localized vibrations occuring on a fast timescale in between the jumps. We assume that vibrations are Gaussian and distributed according to $f_{\rm vib}(r) = (2\pi\ell^2)^{-3/2}\exp(-r^2/2\ell^2)$, so that ℓ^2 represents the variance of the size of vibrations. We also assume that the jump size is distributed according to $f_{\rm jump}(r) = (2\pi d^2)^{-3/2}\exp(-r^2/2d^2)$, introducing d^2, the variance in the size of the jumps. The last ingredient needed to define the CTRW model is the distribution of times between jumps, called the waiting time distribution [22], which we denote as

$\phi_2(t)$, for reasons that will become clear in a moment.

With these definitions, one can express the van Hove function as [22]

$$G_s(r,t) = \sum_{n=0}^{\infty} p(n,t) f(n,r), \tag{2}$$

where $p(n,t)$ is the probability to make n jumps in a time t, and $f(n,r)$ is the probability to move a distance r in n jumps [22]. These probabilities involve convolutions and are more easily expressed in the Fourier-Laplace domain, $(r,t) \rightarrow (q,s)$. The sum in Eq. (2) is geometric and can be performed easily to yield the well-known result [27]:

$$G_s(q,s) = f_{\rm vib}(q)\frac{1-\phi_1(s)}{s} + f(q)f_{\rm vib}(q)\frac{\phi_1(s)}{s}\frac{1-\phi_2(s)}{1-\phi_2(s)f(q)}, \tag{3}$$

where we defined $f(q) \equiv f_{\rm vib}(q) f_{\rm jump}(q)$ and the distribution $\phi_1(t)$ is related to the waiting time distribution $\phi_2(t)$ through the Feller relation [27]:

$$\phi_1(t) = \frac{\int_t^\infty dt' \phi_2(t')}{\int_0^\infty dt' \phi_2(t') t'}. \tag{4}$$

Physically, $\phi_1(t)$ represents the distribution of the time, t, a walker takes to undergo a jump starting from an arbitrary initial condition at time $t = 0$. Note that ϕ_1 becomes equal to ϕ_2 when the distribution of waiting time is a simple exponential, while it also follows that the moments of $\phi_1(t)$ are larger than those of $\phi_2(t)$ if the distributions are broader than exponential [28, 29, 30]. In a measurement of the van Hove function, $\phi_1(t)$ represents the distribution of the time to the first observed jump, as seen in the first term in the right hand side of Eq. (3), corresponding to $n = 0$ in Eq. (2). The distribution $\phi_2(t)$ quantifies the time between subsequent jumps and contributes to the second term in Eq. (3) which contains the contribution of all the terms with $n > 0$ in the sum (2).

The importance of the distinction between the first and subsequent jumps in order to derive the correct expression of the van Hove function was emphasized long ago by Tunaley [27], and is crucial when the distribution of waiting time becomes broad. As noted by Monthus and Bouchaud [20], and by Barkai and coworkers [28, 29], this first term is in fact directly responsible of the aging dynamics observed in CTRW characterized by "fat" waiting time distributions. In Ref. [29], Barkai *et al.* even provide an example of a system for which the average time to the first jump is infinite, while the average time between jumps is finite: Eq. (3) then shows that in that case particles never leave their initial positions. Jung *et al.* [23, 31] refer to the two distributions as "persistence" and "exchange" and relate them to the decoupling phenomena observed in supercooled liquids.

To proceed further and use Eq. (3) to fit experimental or numerical data, one needs input about the waiting time distribution. It has been claimed by Odagaki and Hiwatari [19] that waiting time distributions in a binary mixture of soft spheres becomes fat with power law tails at low temperature, as in the trap models studied of Monthus and Bouchaud [20]. Garrahan and coworkers performed extensive studies of waiting time distributions both in kinetically constrained glass models [23, 30] and more recently using molecular dynamics simulations [31]. Their results clearly confirm that waiting time distributions in glass-forming systems are not trivial. In particular, they report measurements of various moments of the distributions ϕ_1 and

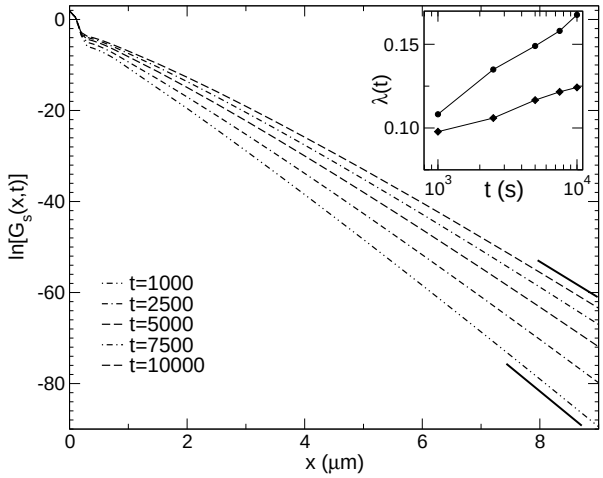

Figure 4. Self-part of the van Hove function predicted by the model in Eq.(3) with parameters $t_1 = 3 \times 10^5$ s, $t_2 = 10^4$ s, $\ell = 0.08\mu m$ and $d = 0.284\mu m$ at different times t. We show the data on an extended vertical scale to show that the tail is indeed very close to being exponential. Inset: Fitted slope λ for different precision measurements, $G_s(r,t) \approx 10^{-5}$ (top) and $G_s(r,t) \approx 10^{-30}$ (bottom). The very slow growth simply reflects crossover towards the long-time Gaussian form of the distribution at fixed x.

ϕ_2 and confirm that they evolve differently with temperature [30, 31], establishing the complex nature of the waiting time distributions for glass-formers.

Using these insights, we have suggested [16] the following simplification to make the use of Eq. (3) much more practical. In the absence of definite information on the detailed shape of $\phi_2(t)$, we characterize $\phi_1(t)$ and and $\phi_2(t)$ in Eq. (3) by their respective first moments, t_1 and t_2, and we generally expect that

$$t_2 \leq t_1. \tag{5}$$

We assume that the distributions $\phi_1(t)$ and $\phi_2(t)$ are exponential, $\phi_1(t) = t_1^{-1} \exp(-t/t_1)$ and $\phi_2(t) = t_2^{-1} \exp(-t/t_2)$, and that they are independent from one another. The real link between them in the Feller relation (4) and their complex shapes are now hidden in the inequality (5).

3.3. The exponential tail

The first term in Eq. (3), which corresponds to the particles undergoing localized vibrations modulated by the waiting time distribution for first jumps, controls the shape of the central part of the van Hove function $G_s(x,t)$. The second term in Eq. (3) is responsible for the broad tail in $G_s(x,t)$ and stems from particles which have performed one or several jumps after a time t. Using parameters relevant for our colloidal system (see below for the details of the fitting procedure), we present on an extended vertical scale, the predictions of Eq. (3) concerning the shape of the van Hove function and its evolution with time in Fig. 4. The van Hove functions can

clearly be described as the superposition of "mobile" and "immobile" particles with broad tails that are well fitted by an exponential decay for large x:

$$G_s(x,t) \sim \exp\left(-\frac{x}{\lambda(t)}\right), \tag{6}$$

which defines a new lengthscale $\lambda(t)$.

In fact, a close to exponential decay of the van Hove function is present in the original CTRW model [22] when distances outside the realm of central limit theorem are considered. Using a saddle-point calculation, we have proved [16] analytically that Eq. (3) generically leads to broad distributions that indeed decay exponentially (with logarithmic corrections). Interestingly this expansion can be obtained independently of the actual shape of the distributions, establishing its universality. We have also shown [16] that these tails simply become enhanced in glassy materials, and are therefore more easily measured using typical experimental accuracy.

Using the exact solution from Eq. (3) shown in Fig. 4, we fit the decay of $G_s(x,t)$ with an exponential function for two measurements of different precisions corresponding to G_s levels of 10^{-5} as in typical experiments, and of 10^{-30}, which is obviously not accessible experimentally. We find that the lengthscale $\lambda(t)$ slowly increases with time, the growth being slower for the most asymptotic measurements. This suggests that if one were to measure $\lambda(t)$ for even lower values of $G_s(x,t)$, $\lambda(t)$ would be almost constant, in agreement with the saddle-point calculation. In fact, most of the time dependence of $\lambda(t)$ observed through fitting is due to the distribution crossing over, at fixed x and increasing t, to its long-time Gaussian limit. We conclude therefore that probably the "growing lengthscale" $\lambda(t)$ does not carry any deep physical information.

Finally we remark that, quite often, the quantities $4\pi r^2 G_s(r,t)$ or even $P(\log_{10} r, t) \propto r^3 G_s(r,t)$ are measured in simulations [14, 17], and the appearance of a secondary peak in r at low temperature is given a large significance, supposedly signalling the change towards an "activated" dynamics with "hopping" processes. We would like to inform that within our CTRW model (which is a purely "hopping" model), a secondary peak is not necessarily present. Although the functions $r^2\exp(-r/\lambda)$ and $r^3\exp(-r/\lambda)$ describing the tails have a maximum at some value of r, this peak is sometimes buried below the Gaussian central part of the van Hove function, so that only a shoulder (instead of a secondary maximum) is observed. A peak emerges, for instance, when the ratio between times t_1 and t_2 is large enough, the precise limiting value depending also on the parameters d and ℓ. Therefore, we believe that the observation of such peaks is not in general indicative of a deep change in the physical behaviour of the system.

3.4. Fitting the data

We have used the model, given by Eq. (3), with the four fitting parameters $\{d, \ell, t_1, t_2\}$ described above to fit the van Hove function $G_s(x,t)$ measured in our experimental system. Like in our previous work with different materials showing slow dynamics [16], suitable choice of the fitting parameters results in very good fits of the experimental data, as can be recognized from Fig. 2. The fitting parameters we have used are presented in Table 1.

To confirm that the good agreement obtained from the model is not due to a large number of free parameters that would allow to fit any set of data, we have tried

ϕ	ℓ	d	$t_1^{\rm th}$	$t_2^{\rm th}$	$t_1^{\rm exp}$	$t_2^{\rm exp}$
0.37	0.14	0.195	300	70	59	36
0.403	0.10	0.251	4000	800	955	448
0.429	0.08	0.279	60000	5000	11050	4047
0.440	0.06	0.284	300000	10000	22300	7086

Table 1. Fitting parameters used to get the fits shown in Fig. 2. Timescales are in seconds, lengthscales in microns.

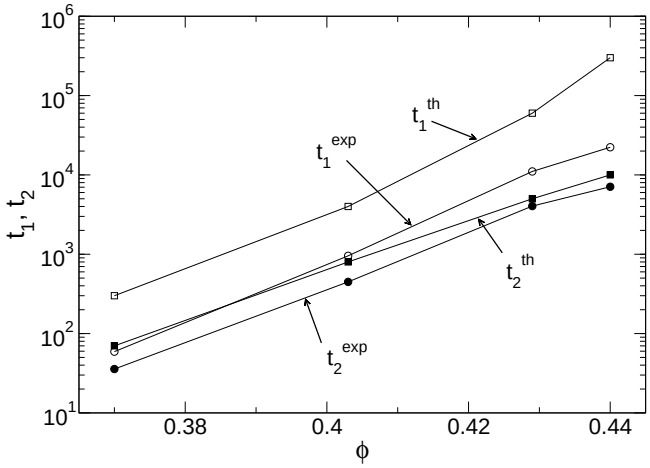

Figure 5. The times t_1 and t_2 obtained directly from experiments "exp" are compared to the timescales obtained through the fitting procedure "th". The ϕ dependence of both sets of data is similar, and the inequality $t_1 > t_2$ is strong in both cases, indicative of a broad distribution of waiting times $\phi_2(t)$.

to compare our choice for the waiting times, t_1 and t_2, with the same quantities being measured directly from the observed trajectories.

To do so, we must determine the "jumps" from our trajectories. In our experiments, we say that a particle undergoes a jump if the magnitude of its displacement between two successive experimental frames is larger than a threshold, $x_{\rm cut}$. Here we consider displacements only in one dimension, and use $x_{cut} = 0.1$ μm, which is slightly larger than the typical lengthscale for the vibrations, $x_{\rm cut} > \ell$. Similar to the CTRW model, we measure two distinct timescales associated with the jumps and separately record timescales to the first jump from an arbitrary initial condition, and timescales between jumps. Given that our experimental trajectories have a finite duration, we observe particles which do not jump, meaning that we probably underestimate both timescales. Moreover, it needs to be noted that in the present experiment, only trajectories where at least two jumps have occured are being recorded meaning that t_1 is slightly more underestimated than t_2 in our measurements. From the statistics of the observed events, we obtain two time distributions, from which we compute the first moments, which we label as $t_1^{\rm exp}$ and $t_2^{\rm exp}$, respectively.

We can then compare the experimental data to the results obtained through the

fitting procedure, which we label as $t_1^{\rm th}$ and $t_2^{\rm th}$, as shown in Fig. 5. We find that the average waiting times, measured directly from experiments and by using the CTRW fitting procedure, show very similar trends when volume fraction is varied. This good agreement gives evidence that our modeling of the dynamics is physically correct, and that our fitting procedure of the van Hove function indeed yields a detailed statistical information on the particle trajectories.

However, the numbers for t_1 and t_2 obtained from the CTRW model are higher than the numbers extracted from experimental measurements by a factor 2 and 10, respectively. There can be several reasons for this mismatch, which might originate from the model or from the experimental determination of waiting times, or from both. The waiting time distributions are perhaps far more complex than the exponential distributions that are used in our model. But, as mentioned above, we have good reasons to believe that waiting times are slightly underestimated in our experimental analysis, t_1 more than t_2, a trend compatible with Fig. 5. One could also imagine the presence of back and forth motions, as seen in Fig. 3, and that would erroneously be counted as jumps, again biasing the experimental waiting times towards small values, in agreement with the results presented in Fig. 5. Given these possible sources of discrepancy, we conclude that the agreement reported in Fig. 5 is quite satisfactory.

4. Conclusion

In this paper, we have analyzed the heterogeneous dynamics of a colloidal system which undergoes dynamical arrest at a volume fraction intermediate between low density gels and dense glasses. We have focused our attention on single particle trajectories and have analyzed in detail the self-part of the van Hove distribution functions. These distributions are strongly non-Gaussian with tails that are broad and decay close to exponentially with distance. We have shown that a simple continuous time random walk analysis proposed in the context of glass and jamming transitions describes the experimental data in a very satisfactory manner, showing that the present experimental system shares deep similarities with other glassy systems.

Acknowledgments

We thank J. Röttler and M. Kennett for inviting us to participate to the workshop "Mechanical behaviour in glassy behaviour", Vancouver, July 21-23, 2007, which led to the present collaborative work. We would also like to thank David Reichman and Andreas Heuer for useful correspondence. Financial support from the Joint Theory Institute (Argonne National Laboratory and University of Chicago), CEFIPRA Project 3004-1, and ANR Grants TSANET and DYNHET is acknowledged.

References

[1] A. N. Adhikari, N. A. Capurso, and D. Bingemann, J. Chem. Phys. **127**, 114508 (2007).
[2] E. Vidal Russell and N. E. Israeloff, Nature **408**, 695 (2000).
[3] W. K. Kegel and A. van Blaaderen, Science **287**, 290 (2000).
[4] E. R. Weeks, J. C. Crocker, A. C. Levitt, A. Schofield, and D. A. Weitz, Science **287**, 627 (2000).
[5] G. Marty and O. Dauchot, Phys. Rev. Lett. **94**, 015701 (2005).
[6] P. Bursac, G. Lenormand, B. Fabry, M. Oliver, D. A.Weitz, V. Viasnoff, J. P. Butler, and J. J. Fredberg, Nat. Mater. **4**, 557 (2005).
[7] L. J. Kaufman and D. A. Weitz, J. Chem. Phys. **125**, 074716 (2006).

[8] A. S. Keys, A. R. Abate, S. C. Glotzer, and D. J. Durian, Nature Phys. **3**, 260 (2007).
[9] Y. Gao and M. Kilfoil, Phys. Rev. Lett. **99**, 078301 (2007).
[10] C. J. Dibble, M. Kogan, and M. J. Solomon, Phys. Rev. E **74**, 041403 (2006).
[11] M. D. Ediger, Annu. Rev. Phys. Chem. **51**, 99 (2000).
[12] E. Zaccarelli, J. Phys.: Condens. Matter **19**, 323101 (2007).
[13] S. Manley, H. M. Wyss, K. Miyazaki, J. C. Conrad, V. Trappe, L. J. Kaufman, D. R. Reichman, and D. A. Weitz, Phys. Rev. Lett. **95**, 238302 (2005).
[14] A. M. Puertas, M. Fuchs, and M. E. Cates, J. Chem. Phys. **121**, 2813, (2004).
[15] P. Hurtado, L. Berthier, and W. Kob, Phys. Rev. Lett. **98**, 135503 (2007).
[16] P. Chaudhuri, L. Berthier, and W. Kob, Phys. Rev. Lett. **99**, 060604 (2007).
[17] W. Kob, C. Donati, S. J. Plimpton, P. H. Poole, and S. C. Glotzer, Phys. Rev. Lett. **79**, 2827 (1997).
[18] D. A. Stariolo and G. Fabricius, J. Chem. Phys. **125**, 064505 (2006).
[19] T. Odagaki and Y. Hiwatari, Phys. Rev. A **41**, 929 (1990).
[20] C. Monthus and J.-P. Bouchaud, J. Phys. A **29**, 3847 (1996).
[21] L. Berthier, D. Chandler, and J. P. Garrahan, Europhys. Lett. **69**, 320 (2005).
[22] E. W. Montroll and G. H. Weiss, J. Math. Phys. (N.Y.) **6**, 167 (1965).
[23] Y. Jung, J.P. Garrahan, and D. Chandler, Phys. Rev. E **69**, 061205 (2004).
[24] L. Berthier and W. Kob, J. Phys.: Condens. Matter **19**, 205130 (2007).
[25] J. S. Langer and S. Mukhopadhyay, arXiv:0704.1508.
[26] L. Berthier and R. L. Jack, Phys. Rev. E **76**, 041509 (2007).
[27] J. K. E. Tunaley, Phys. Rev. Lett. **33**, 1037 (1974).
[28] E. Barkai and Y.-C. Cheng, J. Chem. Phys. **118**, 6167 (2003).
[29] E. Barkai, V. Fleurov, and J. Klafter, Phys. Rev. E **61**, 1164 (2000).
[30] Y. Jung, J. P. Garrahan, and D. Chandler, J. Chem. Phys. **123**, 084509 (2005).
[31] L. O. Hedges, L. Maibaum, D. Chandler, and J. P. Garrahan, J. Chem. Phys. **127**, 211101 (2007).